ACADEMIC PRESS

Available online at www.sciencedirect.com

SCIENCE DIRECT®

Journal of Sound and Vibration 261 (2003) 613–633

JOURNAL OF SOUND AND VIBRATION

www.elsevier.com/locate/jsvi

Development of vibration signature analysis using multiwavelet systems

S.E. Khadem[a,*], M. Rezaee[b]

[a] *Mechanical Engineering Department, Tarbiat Modarres University, P.O. Box 14115-177, Tehran, Iran*
[b] *Mechanical Engineering Department, Faculty of Engineering, Tabriz University, Tabriz, Iran*

Received 2 March 2001; accepted 30 April 2002

Abstract

In this paper the vibration analysis for local faults and transient phenomena detection, using multiwavelet systems, is developed. Unlike the scalar wavelet systems, in which their coefficients are scalar parameters, the transformation coefficients of multiwavelet systems are vector valued, and their calculation requires specialized techniques. In this investigation, having considered the technique used to obtain the scalar wavelet system coefficients, the transformation coefficients of the multiwavelet system are calculated, and by applying the method to artificial vibration signals, decomposition of the signal into different multiscale and multiwavelet functions (as introduced by Donovan, Geronimo, Hardin and Massopust) is examined, as well as the capability of this multiwavelet system for transient phenomena detection. By analyzing the vibration signal of a faulty gearing system the applicability of Donovan, Geronimo, Hardin and Massopust multiwavelet system for local fault detection of the mechanical systems is shown. The results confirm that using the multiwavelet system, not only can the fault in the gearing system be diagnosed, but also its location can be determined precisely.

1. Introduction

During the last decade, the wavelet systems have been introduced as a new technique for signal analysis applications. Among the others, Daubechies wavelet system using a single basic scaling function and its associated wavelet function as analyzing functions, is one of the most popular wavelet systems [1–3]. One of the main aspects of these systems, is the orthogonality of the scale and wavelet functions.

*Corresponding author.
E-mail address: khadem@modares.ac.ir (S.E. Khadem).

0022-460X/03/$ - see front matter
doi:10.1016/S0022-460X(02)00992-6

Recently, some researchers have investigated the applicability of using several scale and wavelet functions, named multiwavelet systems. The multiwavelet systems have more desirable properties, such as symmetry of the scale functions, which cannot be obtained through the scalar wavelet systems. Geronimo et al. [4] obtained two symmetric orthogonal scaling functions for the first time. Using these multiscale functions, Strang and Strela [5] and Donovan et al. [6] obtained a set of multiwavelet system with two wavelet functions. One of these wavelet functions is symmetric and the other antisymmetric.

In the few past years, many researchers have investigated the applicability of scalar wavelet systems to analyze the vibrational signals of mechanical systems, such as gearboxes and rolling element bearings [7–13]. More recently, several investigations have been performed to increase the capability of wavelet systems, and many researchers have used multiwavelet systems, especially the DGHM[1] multiwavelet system, in applications such as data compression, image processing, noise reduction, as well as data preprocessing in order to perform the multiwavelet transform on a given signal [14–23].

Although several investigations have been performed on the applicability of scalar wavelet systems to vibration signature analysis for fault detection of mechanical systems, multiwavelet systems have not been used to analyze the vibration signals for fault detection so far. In this paper for the first time, the analysis of vibration signals using the DGHM multiwavelet system is investigated for local faults and transient phenomena detection in mechanical systems.

Here, the theoretical bases of multiwavelet systems is examined. For this purpose, the relationship between the multiscale and multiwavelet function spaces which generate a multiresolution analysis is considered, and then, the manner of developing the notion of multiresolution analysis of scalar wavelet systems to multiwavelet systems with several scale and wavelet functions is represented. The main difference between the multiresolution analysis of a scalar wavelet system and a multiwavelet system is the number of spaces spanned by the scale and wavelet functions of the mentioned systems. Unlike the scalar wavelet systems, where the signal space is generated using the shifting and dilation of a single scale and wavelet function, called mother scaling function and mother wavelet function, in the multiwavelet case, the signal space is constructed by shifting and dilation of several scale and wavelet functions.

In order to use the multiwavelet systems to analyze the vibration signals, one has to obtain the coefficients of the multiwavelet systems, but in these systems due to multiplicity of scale and wavelet functions, the multiwavelet transform coefficients are vector-valued parameters. In this case the method of obtaining the scalar wavelet transform coefficients is not applicable, and one needs to perform another scheme. In this paper, an elegant scheme for generalization of scalar wavelet transform to the multiwavelet systems is proposed. Using the DGHM multiwavelet system and applying the proposed scheme, some artificial vibrational signals are analyzed, and the capability of the multiwavelet system for transient phenomena detection and the other phenomena hidden in the signal is studied. In order to show the ability of the multiwavelet system for fault detection of gearboxes, the vibration signal of a gearing system with a cracked tooth is analyzed.

[1] A multiwavelet system introduced by G.C. Donovan, J.S. Geronimo, D.P. Hardin and P.R. Massopust is known as DGHM multiwavelet system, and DGHM refers to their initials.

The results show that the transient phenomena due to the presence of defects, could be diagnosed very efficiently using the multiwavelet systems. Diagnosing the presence of a local fault in a gearbox is the first stage for damage detection and determination of the location of the damaged tooth is more important. Therefore, it is shown that by having a tacho signal as a reference and using the multiwavelet system, one could determine the damaged tooth of the gear.

2. Introduction to multiscale and multiwavelet functions

Using the scalar wavelet systems, the signal space is spanned by the dilation and translation of a single function, but the multiwavelet systems use a vector-valued function Φ which has r scale functions φ_r, $r \in N$ as its elements:

$$\mathbf{\Phi} = [\varphi_1 \varphi_2 \dots \varphi_r]^{\mathrm{T}} \tag{1}$$

and the space generated by the dilation and translation of these functions will be

$$V_j = \overline{\operatorname{span}\{2^{j/2}\varphi_i(2^j t - k) : 1 \leqslant i \leqslant r, k \in Z\}}. \tag{2}$$

In the above equation, the integer j shows the scale of the function φ_i, e.g., $j = 0$ corresponds to the scale function in its normal shape (without any dilation), and by increasing the variable j, the function will be compressed. The shifting of the function φ_i on the time axis is performed by the variable k. The variation of k allows the function to have an arbitrary location on the time axis.

If the following conditions hold among the mentioned spaces, then $\mathbf{\Phi}$ will be the multiscale function [4,20]

$$\cdots \subset V_{-1} \subset V_0 \subset V_1 \subset \cdots, \quad \bigcup_{j \in Z} V_j = L^2(R), \quad \bigcap_{j \in Z} V_j = \{0\},$$
$$f(t) \in V_j \Leftrightarrow f(2t) \in V_{j+1} \quad \forall j \in Z. \tag{3a–d}$$

In this case, the multiscale function $\mathbf{\Phi}$ generates a multiresolution analysis with the multiplicity of r, for $L^2(R)$. By considering the condition

$$\varphi_1(t), \dots, \varphi_r(t) \in V_0 \subset V_1, \tag{4}$$

one could obtain a sequence of matrices $[\mathbf{G}_k]_{k \in Z} \in l^2(Z)^{r \times r}$ such that

$$\mathbf{\Phi}(t) = \sum_{k \in Z} \mathbf{G}_k \mathbf{\Phi}(2t - k). \tag{5}$$

In the other words, the multiresolution analysis equation may be written as

$$\begin{bmatrix} \varphi_1(t) \\ \varphi_2(t) \\ \vdots \\ \varphi_r(t) \end{bmatrix} = \sum_{k \in Z} \begin{bmatrix} g_{11}^k & g_{12}^k & \cdots & g_{1r}^k \\ g_{21}^k & g_{22}^k & \cdots & g_{1r}^k \\ \vdots & \vdots & & \vdots \\ g_{r1}^k & g_{r2}^k & \cdots & g_{rr}^k \end{bmatrix} \begin{bmatrix} \varphi_1(2t - k) \\ \varphi_2(2t - k) \\ \vdots \\ \varphi_r(2t - k) \end{bmatrix}. \tag{6}$$

Eqs. (5) and (6) show that the scale functions at a given resolution can be represented as a linear combination of integer translations of the scale functions at a higher resolution. Therefore, the scale functions can be obtained recursively using the above equations.

If Eq. (5) is written for the various parameters of $t-l, l \in Z$ then the multiresolution relation could be written in a more useful form as

$$\begin{aligned}
&\vdots \\
&\mathbf{\Phi}(t+1) = \sum_{k\in Z} \mathbf{G}_k \mathbf{\Phi}(2(t+1)-k), \quad \mathbf{\Phi}(t) = \sum_{k\in Z} \mathbf{G}_k \mathbf{\Phi}(2t-k), \\
&\mathbf{\Phi}(t-1) = \sum_{k\in Z} \mathbf{G}_k \mathbf{\Phi}(2(t-1)-k), \\
&\vdots
\end{aligned} \tag{7}$$

and one may write the above equation in a compact form as

$$\begin{bmatrix} \vdots \\ \mathbf{\Phi}(t+1) \\ \mathbf{\Phi}(t) \\ \mathbf{\Phi}(t-1) \\ \vdots \end{bmatrix} = \begin{bmatrix} & \vdots & \vdots & \vdots & \\ \cdots & \mathbf{G}_1 & \mathbf{G}_2 & \mathbf{G}_3 & \cdots \\ \cdots & \mathbf{G}_{-1} & \mathbf{G}_0 & \mathbf{G}_1 & \cdots \\ \cdots & \mathbf{G}_{-3} & \mathbf{G}_{-2} & \mathbf{G}_{-1} & \cdots \\ & \vdots & \vdots & \vdots & \end{bmatrix} \begin{bmatrix} \vdots \\ \mathbf{\Phi}(2t+1) \\ \mathbf{\Phi}(2t) \\ \mathbf{\Phi}(2t-1) \\ \vdots \end{bmatrix}, \tag{8}$$

where the $\mathbf{G}_i$'s are $r \times r$ matrices, and to obtain the multiscale functions, one needs to know the $\mathbf{G}_i$ matrices. Geronimo et al. [4] obtained a set of these matrices, using fractal functions, as

$$\begin{aligned}
[\mathbf{G}_0] &= \begin{bmatrix} 3/5 & 4\sqrt{2}/5 \\ -1/10\sqrt{2} & -3/10 \end{bmatrix}, \quad [\mathbf{G}_1] = \begin{bmatrix} 3/5 & 0 \\ 9/10\sqrt{2} & 1 \end{bmatrix}, \\
[\mathbf{G}_2] &= \begin{bmatrix} 0 & 0 \\ 9/10\sqrt{2} & -3/10 \end{bmatrix}, \quad [\mathbf{G}_3] = \begin{bmatrix} 0 & 0 \\ -1/10\sqrt{2} & 0 \end{bmatrix}.
\end{aligned} \tag{9}$$

Using the multiresolution analysis relation, these matrices generate two scale functions $\varphi_1(x)$ and $\varphi_2(x)$, and are non-zero only on the intervals $0<x<1$ and $0<x<2$, respectively. These functions and their frequency spectra are shown in Fig. 1. Figs. 1(c) and (d) show that the first scale function, φ_1, is a lowpass filter and the second scale function, φ_2, acts as a bandpass filter.

In the scalar case, it is easy to obtain the basic wavelet function using the basic scale function, since the coefficients of the multiresolution analysis equation used for obtaining the wavelet functions may be obtained in a simple way by changing the signs and the sequence of the coefficients used in the multiresolution analysis equation to obtain the scale function [3,5]. This method is not efficient for multiwavelet systems and one needs to use another method. If V_j is the space generated by the multiscale functions, then for any $j \in Z$, one may set the complement space, W_j, so that

$$V_{j+1} = V_j \oplus W_j. \tag{10}$$

Considering $\mathbf{\Psi}$, the vector of multiwavelets as

$$[\mathbf{\Psi}] = [\psi_1 \quad \psi_2 \quad \cdots \quad \psi_r]^{\mathrm{T}} \in L^2(R)^r, \tag{11}$$

W_j, the space generated by these multiwavelet functions, will be

$$W_j = \overline{\operatorname{span}\{2^{j/2}\psi_i(2^j t-k)\colon 1 \leqslant i \leqslant r, k \in Z\}}. \tag{12}$$

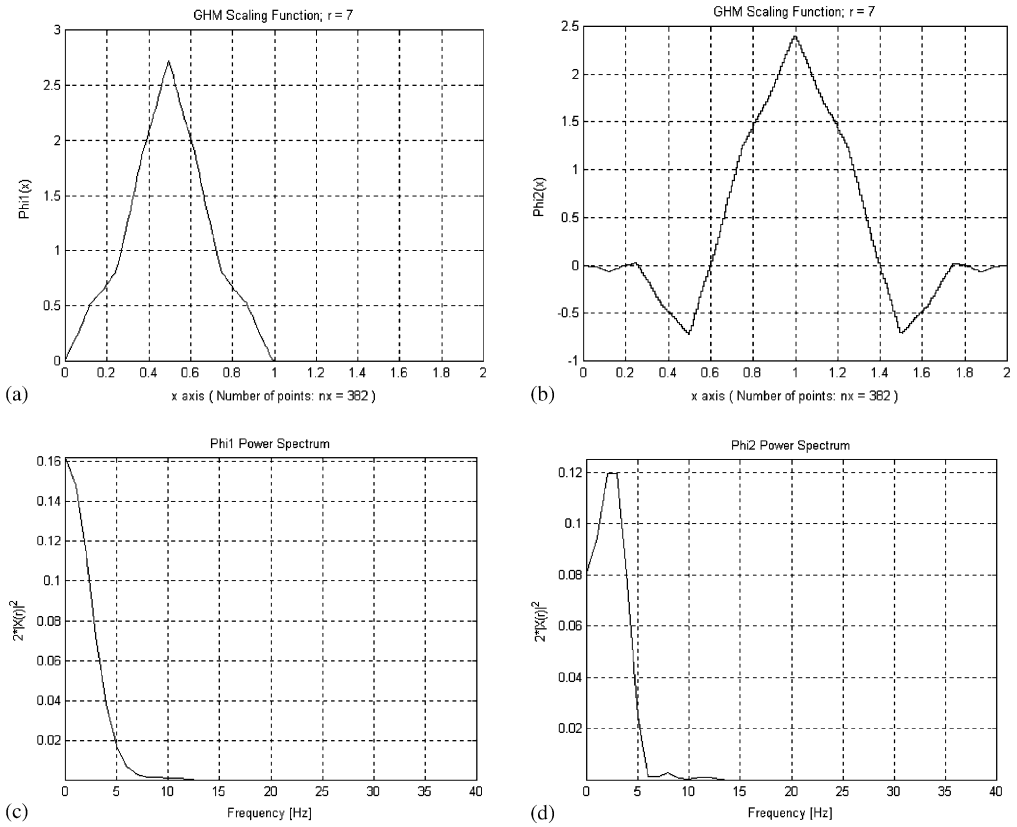

Fig. 1. GHM multiscale functions and their spectra: (a) scale function φ_1, $r = 7$; (b) scale function φ_2, $r = 7$; (c) power spectrum of φ_1; and (d) power spectrum of φ_2.

If $V_j \perp W_j$, and the set $\{2^{j/2}\psi_i(2^j t - k)\colon 1 \leqslant i \leqslant r, k \in Z\}$ forms a stable basis for W_j, and moreover, if the ψ_i's are orthogonal to their integer shifted versions, i.e.,

$$\int \psi_i(t)\psi_j(t-n)\,\mathrm{d}t = \delta_{ij}\delta_n, \tag{13}$$

then the ψ_i's form a set of orthonormal multiwavelet functions satisfying the condition

$$\langle \mathbf{\Psi}(2^j t - n), \mathbf{\Psi}(2^k t - m) \rangle = \delta_{jk}\delta_{nm}\mathbf{I}, \quad j,k,m,n \in Z, \tag{14}$$

where $\mathbf{I}$ is a $r \times r$ identity matrix.

Unlike the scalar case, the coefficients of the multiresolution analysis equation for obtaining the multiwavelet functions are $r \times r$ matrices

$$\mathbf{\Psi}(t) = \sum_{k \in Z} \mathbf{H}_k \mathbf{\Phi}(2t - k). \tag{15}$$

Eq. (15) may be written in the matrix form

$$\begin{bmatrix} \vdots \\ \boldsymbol{\Psi}(t+1) \\ \boldsymbol{\Psi}(t) \\ \boldsymbol{\Psi}(t-1) \\ \vdots \end{bmatrix} = \begin{bmatrix} & \vdots & \vdots & \vdots & \\ \cdots & \mathbf{H}_1 & \mathbf{H}_2 & \mathbf{H}_3 & \cdots \\ \cdots & \mathbf{H}_{-1} & \mathbf{H}_0 & \mathbf{H}_1 & \cdots \\ \cdots & \mathbf{H}_{-3} & \mathbf{H}_{-2} & \mathbf{H}_{-1} & \cdots \\ & \vdots & \vdots & \vdots & \end{bmatrix} \begin{bmatrix} \vdots \\ \boldsymbol{\Phi}(2t+1) \\ \boldsymbol{\Phi}(2t) \\ \boldsymbol{\Phi}(2t-1) \\ \vdots \end{bmatrix}. \tag{16}$$

To obtain the multiwavelet functions, one needs to know the $[\mathbf{H}_i]$ matrices. Strang and Strela [5], and Donovan et al. [6] for the first time obtained a set of these matrices for the case of $r = 2$ as

$$[\mathbf{H}_0] = \frac{1}{10}\begin{bmatrix} -1/\sqrt{2} & -3 \\ 1 & 3\sqrt{2} \end{bmatrix}, \quad [\mathbf{H}_1] = \frac{1}{10}\begin{bmatrix} 9/\sqrt{2} & -10 \\ -9 & 0 \end{bmatrix},$$
$$[\mathbf{H}_2] = \frac{1}{10}\begin{bmatrix} 9/\sqrt{2} & -3 \\ 9 & -3\sqrt{2} \end{bmatrix}, \quad [\mathbf{H}_3] = \frac{1}{10}\begin{bmatrix} -1/\sqrt{2} & 0 \\ -1 & 0 \end{bmatrix}. \tag{17}$$

One obtains the two wavelet functions ψ_1 and ψ_2 using the equation

$$\begin{bmatrix} \psi_1(t) \\ \psi_2(t) \end{bmatrix} = \sum_{k=0}^{3} \begin{bmatrix} h_{11}^k & h_{12}^k \\ h_{21}^k & h_{22}^k \end{bmatrix} \begin{bmatrix} \varphi_1(2t-k) \\ \varphi_2(2t-k) \end{bmatrix}. \tag{18}$$

Fig. 2 shows these multiwavelet functions and their spectra.

As this figure shows, ψ_1 and ψ_2 are symmetric and antisymmetric functions, respectively, and this property cannot be obtained using scalar wavelet systems. As shown in Figs. 2(c) and (d), it is apparent that ψ_1 and ψ_2 are both bandpass filters.

3. Generalization of scalar wavelet transform to multiwavelet systems

Having a multiresolution analysis with multiplicity of r, one may write any given function $f_0 \in L^2(R)$ in terms of multiscale and multiwavelet functions of different levels. If $f_0 \in V_0$, then considering the definition of multiresolution analysis, and applying Eq. (10), one could express V_0 space as

$$V_0 = V_{-1} \oplus W_{-1} = V_{-2} \oplus W_{-2} \oplus W_{-1} = \cdots = V_{-L} \oplus W_{-L} \oplus W_{-L+1} \cdots \oplus W_{-1}, \tag{19}$$

where L is an integer number greater than zero.

Using Eq. (19), any function $f_0 \in V_0$ may be written as a sum of its projections on a space generated by the scale functions and the spaces spanned by the wavelet functions at some levels:

$$f_0 = f_{-1} + g_{-1} = f_{-2} + g_{-2} + g_{-1} = \cdots = f_{-L} + g_{-L} + g_{-L+1} \cdots + g_{-1}. \tag{20}$$

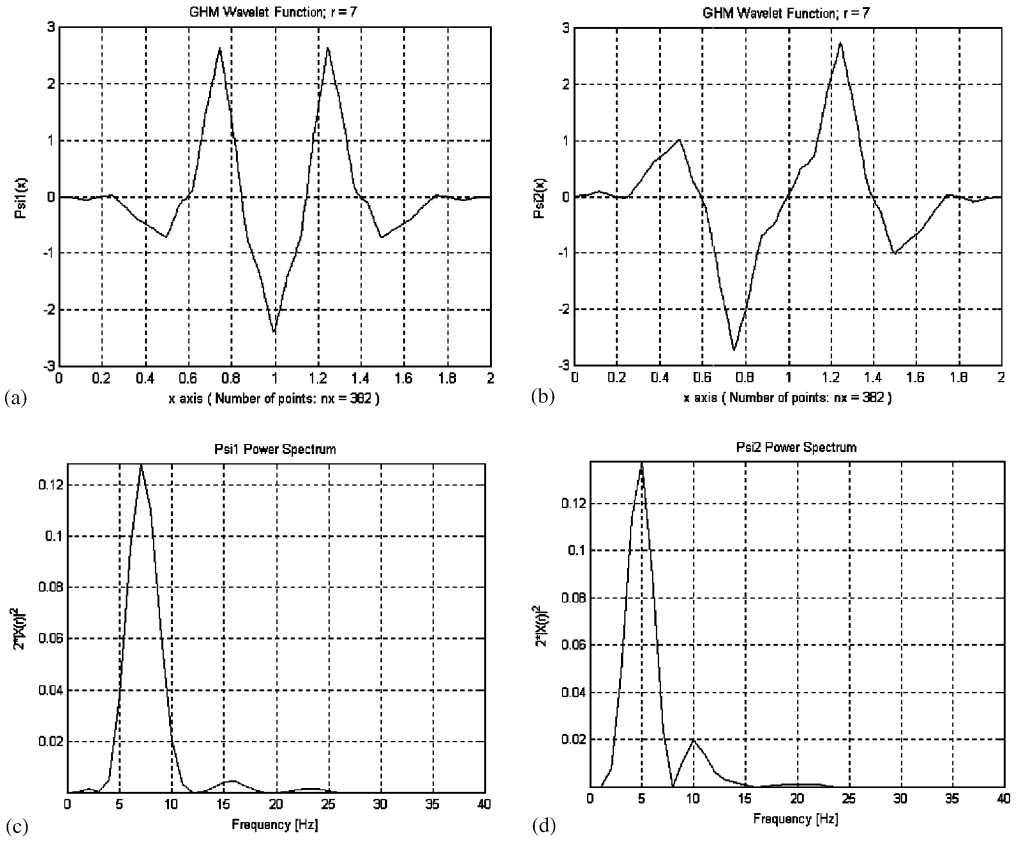

Fig. 2. DGHM multiwavelet functions and their spectra: (a) wavelet function ψ_1, $r = 7$; (b) wavelet function ψ_2, $r = 7$; (c) power spectrum of ψ_1; and (d) power spectrum of ψ_2.

In the above equation, f_{-j} and g_{-j} are the projections of f_0 on V_{-j} and W_{-j} spaces, respectively, i.e.,

$$f_{-j}(t) = \sum_{k\in Z}\sum_{i=1}^{r} c_i^{k,-j}\varphi_i(2^{-j}t-k) = \sum_{k\in Z}(\mathbf{C}_k^{-j})^{\mathrm{T}}\mathbf{\Phi}(2^{-j}t-k), \tag{21}$$

$$g_{-j}(t) = \sum_{k\in Z}\sum_{i=1}^{r} d_i^{k,-j}\psi_i(2^{-j}t-k) = \sum_{k\in Z}(\mathbf{D}_k^{-j})^{\mathrm{T}}\mathbf{\Psi}(2^{-j}t-k). \tag{22}$$

Using Eqs. (19)–(22), one may expand the function $f_0 \in V_0$ as [24]:

$$f_0(t) = \sum_{k\in Z}(\mathbf{C}_k^{0})^{\mathrm{T}}\mathbf{\Phi}(t-k) = \sum_{k\in Z}\{(\mathbf{C}_k^{-L})^{\mathrm{T}}\mathbf{\Phi}(2^{-L}t-k) + (\mathbf{D}_k^{-1})^{\mathrm{T}}\mathbf{\Psi}(2^{-1}t-k) + \cdots + (\mathbf{D}_k^{-L})^{\mathrm{T}}\mathbf{\Psi}(2^{-L}t-k)\}. \tag{23}$$

In order to obtain a relation between $\mathbf{C}_k$'s and $\mathbf{D}_k$'s at two successive levels, one use the dilation equation

$$\mathbf{\Phi}(t) = \sum_{n \in Z} \mathbf{G}_n \mathbf{\Phi}(2t - n). \tag{24}$$

In the above equation, after scaling and shifting the time parameter t to $2^j t - k$, and changing variables $m = 2k + n$, one obtains

$$\mathbf{\Phi}(2^j t - k) = \sum_{m} \mathbf{G}_{(m-2k)} \mathbf{\Phi}(2^{j+1} t - m). \tag{25}$$

On the other hand, since the vector-valued functions $\mathbf{\Phi}(2^j t - k)$, $k \in Z$ generate V_j space, then any given function $f(t) \in V_{j+1}$ may be expanded as [24]

$$f(t) = \sum_{k \in Z} (\mathbf{C}_k^{j+1})^{\mathrm{T}} \mathbf{\Phi}(2^{j+1} t - k). \tag{26}$$

Furthermore, because W_j is the orthogonal complement of V_j in V_{j+1}, then

$$V_{j+1} = V_j \oplus W_j, \quad f(t) = \sum_k (\mathbf{C}_k^j)^{\mathrm{T}} \mathbf{\Phi}(2^j t - k) + \sum_k (\mathbf{D}_k^j)^{\mathrm{T}} \mathbf{\Psi}(2^j t - k). \tag{27}$$

The multiwavelet system uses r basic scale functions, for which one may obtain r basic wavelet functions, and form an orthonormal system of functions. Then Eq. (27) may be written as

$$\begin{aligned} f(t) = & \sum_k \begin{bmatrix} c_{k,1}^j & c_{k,2}^j & \cdots & c_{k,r}^j \end{bmatrix} \begin{bmatrix} \varphi_1(2^j t - k) \\ \varphi_2(2^j t - k) \\ \vdots \\ \varphi_r(2^j t - k) \end{bmatrix} \\ & + \sum_k \begin{bmatrix} d_{k,1}^j & d_{k,2}^j & \cdots & d_{k,r}^j \end{bmatrix} \begin{bmatrix} \psi_1(2^j t - k) \\ \psi_2(2^j t - k) \\ \vdots \\ \psi_r(2^j t - k) \end{bmatrix}. \end{aligned} \tag{28}$$

Considering the orthogonality of scale and wavelet functions, one obtains the expansion coefficients, $c_{k,i}^j$ and $d_{k,i}^j$ as

$$c_{k,i}^j = 2^j \langle f(t), \varphi_i(2^j t - k) \rangle, \quad d_{k,i}^j = 2^j \langle f(t), \psi_i(2^j t - k) \rangle. \tag{29a, b}$$

On the other hand, for a multiwavelet system with multiplicity of r, Eq. (25) becomes

$$\begin{bmatrix} \varphi_1(2^j t-k) \\ \varphi_2(2^j t-k) \\ \vdots \\ \varphi_r(2^j t-k) \end{bmatrix} = \sum_m \begin{bmatrix} g_{11}^{(m-2k)} & g_{12}^{(m-2k)} & \cdots & g_{1r}^{(m-2k)} \\ g_{21}^{(m-2k)} & g_{22}^{(m-2k)} & \cdots & g_{2r}^{(m-2k)} \\ \vdots & \vdots & & \vdots \\ g_{r1}^{(m-2k)} & g_{r2}^{(m-2k)} & \cdots & g_{rr}^{(m-2k)} \end{bmatrix} \begin{bmatrix} \varphi_1(2^{j+1}t-m) \\ \varphi_2(2^{j+1}t-m) \\ \vdots \\ \varphi_r(2^{j+1}t-m) \end{bmatrix}, \tag{30a}$$

$$\begin{aligned} \varphi_1(2^j t-k) &= \textstyle\sum_m [g_{11}^{(m-2k)}\varphi_1(2^{j+1}t-m) + g_{12}^{(m-2k)}\varphi_2(2^{j+1}t-m) + \cdots + g_{1r}^{(m-2k)}\varphi_r(2^{j+1}t-m)], \\ \varphi_2(2^j t-k) &= \textstyle\sum_m [g_{21}^{(m-2k)}\varphi_1(2^{j+1}t-m) + g_{22}^{(m-2k)}\varphi_2(2^{j+1}t-m) + \cdots + g_{2r}^{(m-2k)}\varphi_r(2^{j+1}t-m)], \\ &\vdots \\ \varphi_r(2^j t-k) &= \textstyle\sum_m [g_{r1}^{(m-2k)}\varphi_1(2^{j+1}t-m) + g_{r2}^{(m-2k)}\varphi_2(2^{j+1}t-m) + \cdots + g_{rr}^{(m-2k)}\varphi_r(2^{j+1}t-m)]. \end{aligned} \tag{30b}$$

Upon substituting Eq. (30b) in (29a) for $i=1$, one obtains

$$\begin{aligned} & c_{l,1}^j = 2^j[\langle f(t), \sum_m g_{11}^{(m-2l)}\varphi_1(2^{j+1}t-m)\rangle + \cdots + \langle f(t), \sum_m g_{1r}^{(m-2l)}\varphi_r(2^{j+1}t-m)\rangle] \\ & \Rightarrow c_{l,1}^j = 2^j[\sum_m g_{11}^{(m-2l)}\langle f(t), \varphi_1(2^{j+1}t-m)\rangle + \cdots + \sum_m g_{1r}^{(m-2l)}\langle f(t), \varphi_r(2^{j+1}t-m)\rangle], \end{aligned} \tag{31a}$$

$$c_{l,1}^j = \frac{1}{2}\sum_m [\, g_{11}^{(m-2l)} \quad g_{12}^{(m-2l)} \quad \cdots \quad g_{1r}^{(m-2l)}\,] \begin{bmatrix} c_{m,1}^{j+1} \\ c_{m,2}^{j+1} \\ \vdots \\ c_{m,r}^{j+1} \end{bmatrix}. \tag{31b}$$

Using the same approach, one may obtain the $c_{l,i}^j$ coefficients as [24]

$$\begin{bmatrix} c_{l,1}^j \\ c_{l,2}^j \\ \vdots \\ c_{l,r}^j \end{bmatrix} = \frac{1}{2}\sum_m \begin{bmatrix} g_{11}^{(m-2l)} & g_{12}^{(m-2l)} & \cdots & g_{1r}^{(m-2l)} \\ g_{21}^{(m-2l)} & g_{22}^{(m-2l)} & \cdots & g_{2r}^{(m-2l)} \\ \vdots & \vdots & & \vdots \\ g_{r1}^{(m-2l)} & g_{r2}^{(m-2l)} & \cdots & g_{rr}^{(m-2l)} \end{bmatrix} \begin{bmatrix} c_{m,1}^{j+1} \\ c_{m,2}^{j+1} \\ \vdots \\ c_{m,r}^{j+1} \end{bmatrix}. \tag{32a}$$

Considering the fact that the G_i's matrices corresponding to the DGHM multiwavelet system are 2×2 matrices (i.e., $r=2$), then the above equation for the DGHM case may be simplified easily as

$$\begin{bmatrix} c_{l,1}^j \\ c_{l,2}^j \end{bmatrix} = \frac{1}{2}\sum_m \begin{bmatrix} g_{11}^{(m-2l)} & g_{12}^{(m-2l)} \\ g_{21}^{(m-2l)} & g_{22}^{(m-2l)} \end{bmatrix} \begin{bmatrix} c_{m,1}^{j+1} \\ c_{m,2}^{j+1} \end{bmatrix}. \tag{32b}$$

Both of the above equations can be written in a compact form as

$$\mathbf{C}_l^j = \frac{1}{2}\sum_m \mathbf{G}_{(m-2l)}\mathbf{C}_m^{j+1}, \tag{33}$$

and similarly, one may prove that the following relation holds between the wavelet and scale function coefficients [24]:

$$\mathbf{D}_l^j = \frac{1}{2}\sum_m \mathbf{H}_{(m-2l)}\mathbf{C}_m^{j+1}. \tag{34}$$

Eqs. (33) and (34) show that how a given signal can be analyzed to its projections on the lower scale spaces. Here, there is a question to be answered.

Is it possible to reconstruct the original signal using its projections on different spaces, and if it is so, how?

The answer is positive, and one needs to consider a signal which is belonging to the space generated by the scale functions at scale $j+1$ as

$$f(t) \in V_{j+1} \tag{35}$$

and can be represented in terms of scale functions at the scale $j+1$,

$$f(t) = \sum_k (\mathbf{C}_k^{j+1})^{\mathrm{T}} \mathbf{\Phi}(2^{j+1}t - k). \tag{36}$$

To expand the signal $f(t)$ at one lower scale, considering the multiresolution analysis equation, one needs the wavelet functions

$$f(t) = \sum_k (\mathbf{C}_k^{j})^{\mathrm{T}} \mathbf{\Phi}(2^{j}t - k) + \sum_k (\mathbf{D}_k^{j})^{\mathrm{T}} \mathbf{\Psi}(2^{j}t - k). \tag{37}$$

By substituting the multiresolution analysis equation in Eq. (37), and applying proper changes of variables, the following equation is obtained:

$$\begin{aligned}\sum_k (\mathbf{C}_k^{j+1})^{\mathrm{T}} \mathbf{\Phi}(2^{j+1}t - k) = {} & \sum_k (\mathbf{C}_k^{j})^{\mathrm{T}} \sum_m \mathbf{G}_{m-2k} \mathbf{\Phi}(2^{j+1}t - m) \\ & + \sum_k (\mathbf{D}_k^{j})^{\mathrm{T}} \sum_m \mathbf{H}_{m-2k} \mathbf{\Phi}(2^{j+1}t - m).\end{aligned} \tag{38}$$

Multiplying Eq. (38) by $\varphi_1(2^{j+1}t - l)$ and integrating the obtained equation, [24]

$$c_{k,1}^{j+1}\left(\tfrac{1}{2^{j+1}}\right)\delta_{kl} = \sum_k (\mathbf{C}_k^{j})^{\mathrm{T}} \begin{bmatrix} g_{11}^{(m-2k)}\left(\frac{1}{2^{j+1}}\right)\delta_{ml} \\ g_{21}^{(m-2k)}\left(\frac{1}{2^{j+1}}\right)\delta_{ml} \\ \vdots \\ g_{r1}^{(m-2k)}\left(\frac{1}{2^{j+1}}\right)\delta_{ml} \end{bmatrix} + \sum_k (\mathbf{D}_k^{j})^{\mathrm{T}} \begin{bmatrix} h_{11}^{(m-2k)}\left(\frac{1}{2^{j+1}}\right)\delta_{ml} \\ h_{21}^{(m-2k)}\left(\frac{1}{2^{j+1}}\right)\delta_{ml} \\ \vdots \\ h_{r1}^{(m-2k)}\left(\frac{1}{2^{j+1}}\right)\delta_{ml} \end{bmatrix} \tag{39}$$

and by simplifying Eq. (39), one obtains

$$c_{l,1}^{j+1} = \sum_k (\mathbf{C}_k^j)^{\mathrm{T}} \begin{bmatrix} g_{11}^{(l-2k)} \\ g_{21}^{(l-2k)} \\ \vdots \\ g_{r1}^{(l-2k)} \end{bmatrix} + \sum_k (\mathbf{D}_k^j)^{\mathrm{T}} \begin{bmatrix} h_{11}^{(l-2k)} \\ h_{21}^{(l-2k)} \\ \vdots \\ h_{r1}^{(l-2k)} \end{bmatrix}. \tag{40}$$

The remaining coefficients $c_{l,2}^{j+1}$, … and $c_{l,r}^{j+1}$ may be obtained in a similar way. One may arrange the obtained equations in a compact form as a vector equation [24]

$$(\mathbf{C}_l^{j+1})^{\mathrm{T}} = \sum_k (\mathbf{C}_k^j)^{\mathrm{T}} \mathbf{G}_{(l-2k)} + \sum_k (\mathbf{D}_k^j)^{\mathrm{T}} \mathbf{H}_{(l-2k)}. \tag{41}$$

Using Eq. (41), the multiwavelet transform coefficients at a given scale in terms of those at one lower scale are obtained. Moreover, using this equation, the original signal may be reconstructed by adding its projections at the lower scales.

Now that the theoretical bases of the multiwavelet systems and multiwavelet analysis have been established, the multiwavelet theory will be used to analyze some typical signals. For this purpose, the remaining discussions will be dedicated to the analysis of some artificial and experimental vibrational signals using the DGHM multiwavelet system.

4. Analysis of a simple sine wave with a broadband pulse

In this section, using the DGHM multiwavelet system, a sinusoidal signal which is combined with a broadband pulse at time $t = 0.8$ s, is analyzed [24]. Fig. 3(a) shows the signal in the time domain and Fig. 3(b) shows the power spectrum of the signal. As it is obvious from Fig. 3(b), the power spectrum diagram contains a spike at frequency 2 Hz corresponding to the predominant frequency of the signal, i.e., the frequency of the sine wave. Unfortunately, this diagram does not show the location of the pulse on the time axis as well as its frequency. Therefore, one needs to use another method. In order, to analyze the signal using the multiwavelet system, one needs to construct an r-dimensional input sequences from the signal.

For the DGHM multiwavelet system, one may repeat the signal to provide the input data stream. The upper part of Fig. 3(c) shows the repeated signal, and the multiwavelet transform of the signal is shown in the lower part of the figure. Although this diagram by itself provides no more information about the signal, one may extract some comprehensive information about the signal by analyzing the signal to various levels. Fig. 3(d) shows that how the signal has been analyzed to different levels. To analyze the signal using the DGHM multiwavelet system, two scale and wavelet functions are used, then there will be two curves at each level, as shown in Fig. 3(d). The method is verified by adding up the projections of the signal at all levels leading to the original signal. In Fig. 3(d) the reconstructed signal $f(t)$ is plotted on the level 0 as a dashed curve. Examination of Fig. 3(d) reveals much important information about the analyzed signal. One could see the effect of the pulse on levels 4–7 in a small interval around $t = 0.8$ s. Since the

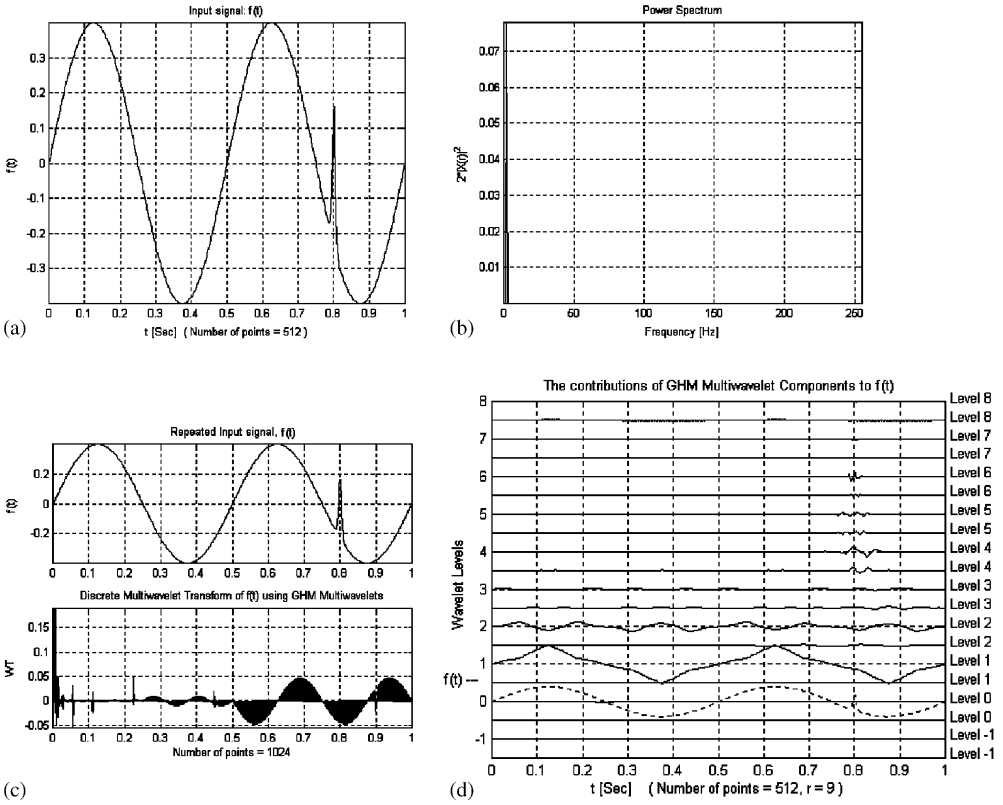

Fig. 3. Analysis of a sinusoidal signal containing a broadband pulse using the DGHM multiwavelet system and frequency analysis method: (a) sinusoidal input signal combined with a broadband pulse; (b) power spectrum of the sinusoidal signal combined with a broadband pulse; (c) repeated input signal (upper) and its multiwavelet transform lower; and (d) projections of the signal at different levels using DGHM multiwavelet system, with the reconstructed signal ($f(E)$). Plotted as a dashed line at lever 0.

perturbation which is occurred at higher levels and covers many wavelet levels, one concludes that the perturbation is due to a transient and broadband phenomenon contained in the signal.

5. Analysis of a sinusoidal signal with varying frequency

A sinusoidal signal with varying frequency, is shown in Fig. 4(a). At first, this signal is analyzed using the frequency analysis method. Fig. 4(b) shows a dB spectrum of the signal. This figure represents the frequency content of the signal covering the frequency band of almost 0–50 Hz. Using this diagram, one cannot obtain any information about the time location of the frequencies. Fig. 4(c) shows the repeated input signal and its multiwavelet transform, and the projections of the signal at different levels of wavelets are shown in Fig. 4(d). Using this figure, one concludes that the input signal has a broadband frequency, as it is found from the frequency analysis method too. Moreover, this figure provides more important information about the signal, i.e., the low-frequency content of the signal are close to time $t = 0$ s, and by increasing the time, the frequency of the signal increases.

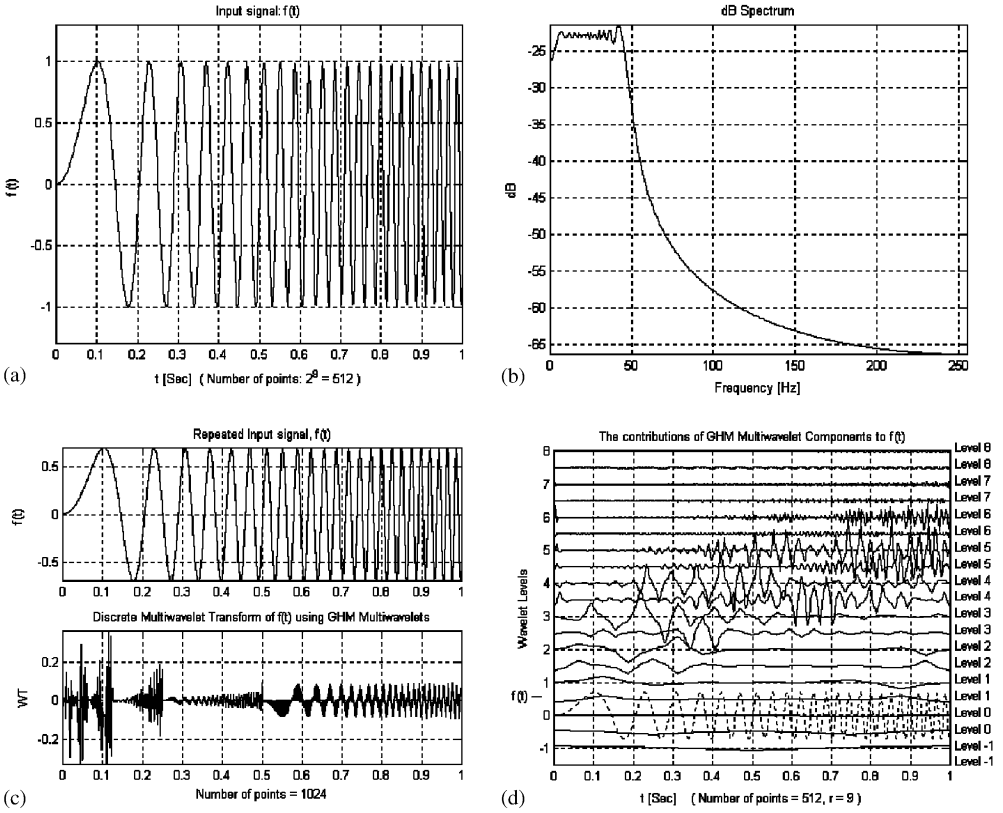

Fig. 4. Analysis of a sinusoidal signal with varying frequency using DGHM multiwavelet system [24]: (a) the sinusoidal signal with varying frequency; (b) dB spectrum of the signal; (c) repeated input signal (upper) and its multiwavelet transform (lower); and (d) analysis of the signal to its projections at different levels of wavelets using the DGHM multiwavelet system.

6. Analysis of a noisy sinusoidal signal combined with a broadband impulse

In this section a sinusoidal signal which is combined with a broadband impulse and contaminated with white noise is analyzed [24]. The signal is shown in Fig. 5(a). The results which are obtained using the spectrum analysis method are shown in Fig. 5(b) as an amplitude spectrum. By considering this diagram, the frequency of the sine wave, the spike at a frequency of about 20 Hz, is obtained easily. Also one notices that the low amplitude spectrum covering the frequency band, results mainly from the presence of white noise. Using this diagram, it is impossible to diagnose the impulse contained in the signal. Moreover, one could not determine the location of the impulse on the time axis using the spectrum analysis method. In order to examine the capability of DGHM multiwavelet system to detect the impulse in the noisy signal, the signal is analyzed using the multiwavelet system. Fig. 5(c) shows the repeated input signal and its DGHM multiwavelet transform. The projections of the signal on different levels are shown in Figs. 5(d)–(f). Upon consideration of Figs. 5(e) and (f), it is obvious that the main part of the broadband pulse manifests itself mainly on levels 6 and 7 of the second wavelet function, ψ_2. Using

Figs. 5(d)–(f), one obtains information about the frequency band and the time location of the impulse contained in the signal. To perform more diagnostic examination to extract the features of the signal, the three-dimensional mean-square map diagram and the two-dimensional contour of the multiwavelet transform coefficients are shown in Figs. 5(g) and (h), respectively. From these figures, the predominant periodic behavior of the signal as well as the presence of the impulse in the signal, is apparent.

7. Identification of a local fault in a gearing system

In this section the capability of the DGHM multiwavelet system for local fault detection of a gearing system is examined. The gearing system consists of two meshing gears each of which has 32 teeth, rotating at a constant speed of about 360 r.p.m. One of the gears has a tooth with a root crack. The vibration signal of the gearing system along with a tacho meter signal are recorded.

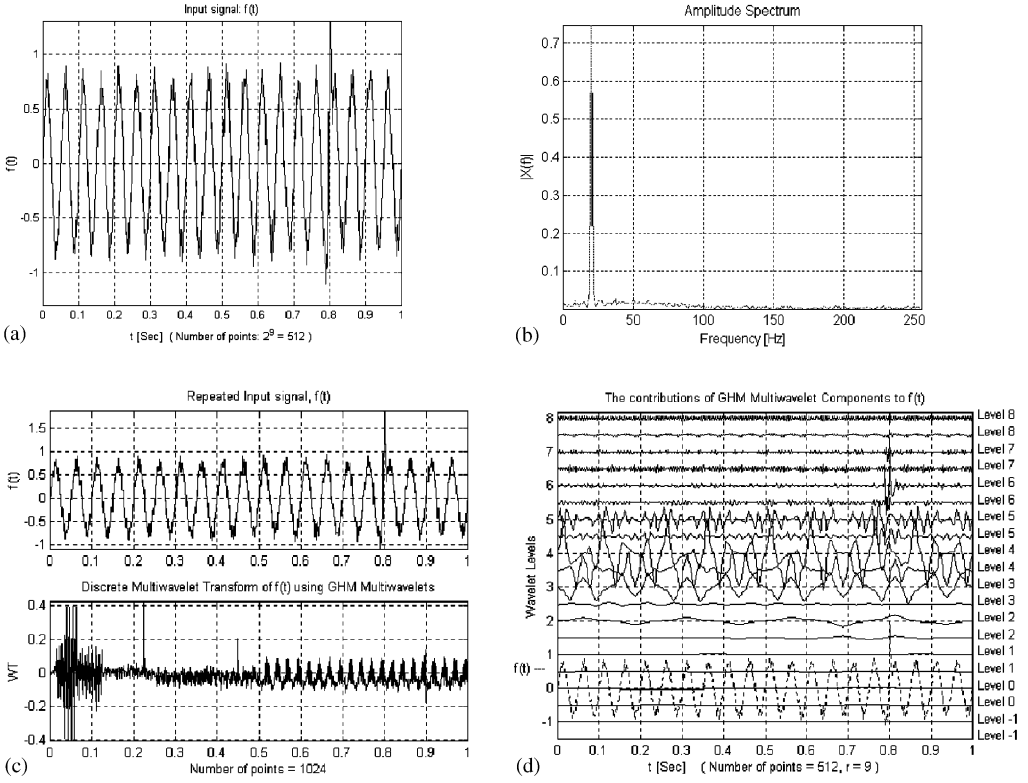

Fig. 5. Analysis of a noisy sinusoidal signal combined with a broadband impulse using DGHM multiwavelet system and the spectrum analysis method: (a) a sinusoidal signal combined with a broadband impulse and white noise; (b) amplitude spectrum of the signal; (c) repeated input signal (upper) and its multiwavelet transform (lower); (d) projections of the signal on different levels analyzed using DGHM multiwavelet system; (e) projections of the signal on different levels of the scale and wavelet functions of φ_1 and ψ_1; (f) projections of the signal on different levels of the scale and wavelet functions of φ_2 and ψ_2; (g) three-dimensional mean-square map diagram of DGHM multiwavelet transform coefficients; and (h) two-dimensional contour diagram of DGHM multiwavelet transform coefficients.

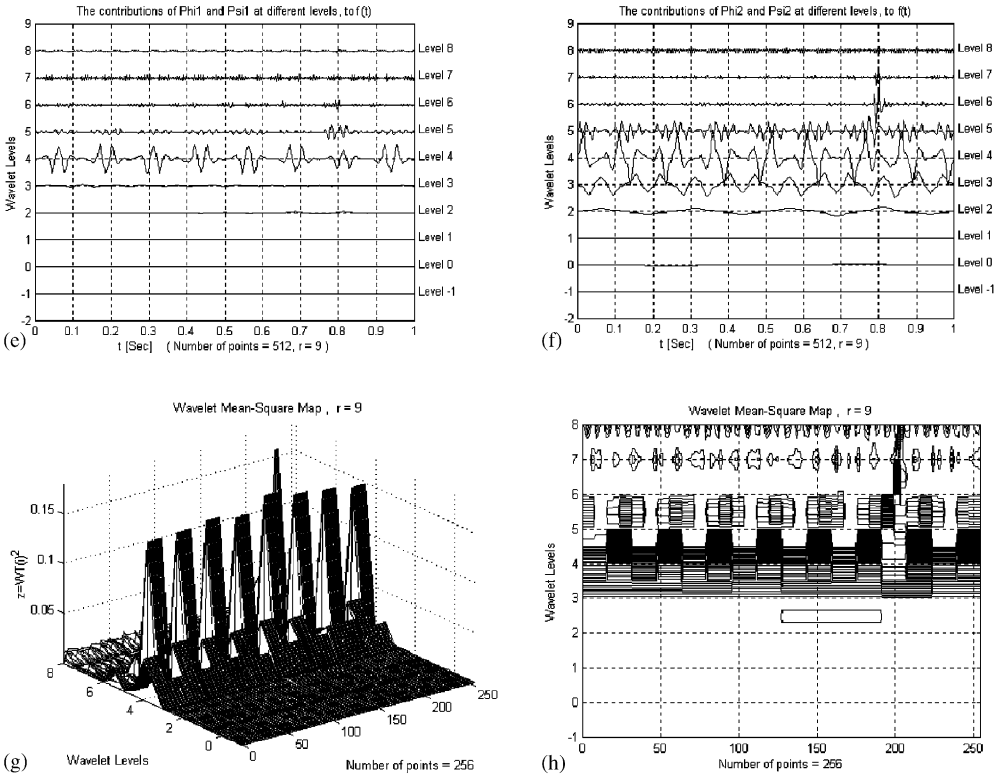

Fig. 5 (*continued*).

The sampling frequency is 24 kHz. Fig. 6 shows the vibration signal of the faulty gear. In order to extract the spectral information, the vibration signal is analyzed using the spectral analysis method. Fig. 7(a) shows the power spectrum of the signal in the range 0–12 kHz. In order to obtain the exact frequencies corresponding to each of the dominant picks, the power spectrum in the range 0–750 Hz is depicted in Fig. 7(b). There are three dominant picks in the spectrum which occur at the frequencies of 5, 190 and 380 Hz, respectively. Considering the shaft speed and the number of teeth on the gears, one concludes that the first peak corresponds to the gear rotational speed, and the second and the third peaks show the gear mesh frequency and its harmonic, respectively. Although the spectrum analysis provides useful information about the described system, using the spectrum itself, one cannot identify the presence and the location of the damage.

The vibration signal of the faulty gear is then analyzed using the DGHM multiwavelet system. The multiwavelet transform of the signal is shown in Fig. 8(a). Fig. 8(b) shows the components of the signal at different levels of the multiscale and the multiwavelet functions. As it is seen from this figure, the signal component at the sixth level of the second wavelet function has an abrupt fluctuation at about 0.065 s. In order to obtain clearer results, the three-dimensional mean-square map corresponding to the scale and wavelet functions φ_1, $\psi_1\varphi_2$ and ψ_2 are shown in Figs. 8(c) and (d), respectively. As these figures show, the presence of the peaks at the sixth level corresponding to the points 95 and 150 are confirmed. However, considering the scale used to show the amplitude of the peaks, one concludes that the peak corresponding to the point 95 is dominant.

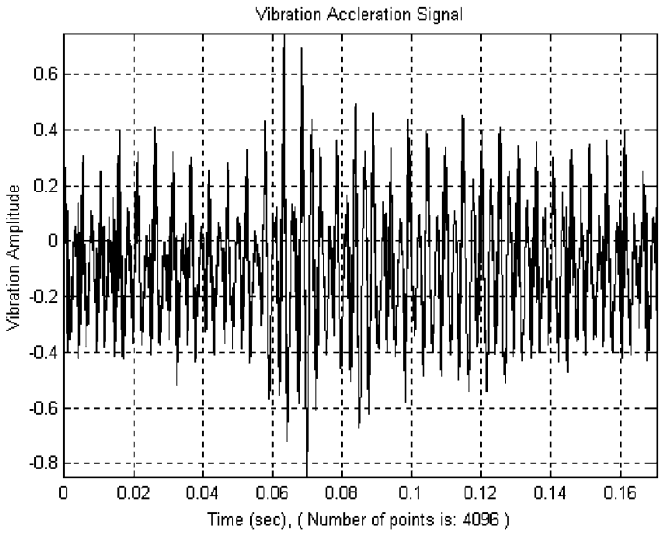

Fig. 6. Vibration signal of a faulty gear.

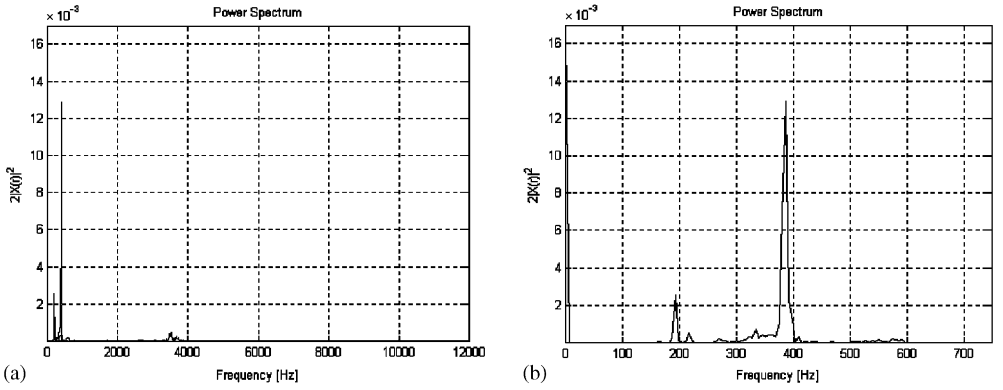

Fig. 7. The spectral analysis of the faulty gear: (a) the power spectrum of the vibration signal of the faulty gear and (b) the power spectrum at the frequency range 0–750 Hz.

Referring to Fig. 8(e) which shows the compound three-dimensional mean-square map of all the scale and wavelet functions of φ_1, φ_2, ψ_1 and ψ_2, the presence of the dominant peak at about the point 95 is verified.

More accurate analysis of the three-dimensional mean-square map shows that the dominant peak is located at the point 95 of the sixth level of wavelet function ψ_2. This point corresponds to the time $t = 0.064$ s at the sixth level of wavelet function ψ_2 in time-scale diagram (Fig. 8(b)).

Now, by having a tacho meter signal as a reference and using the above results, how one can detect the cracked tooth on the gear. Considering that the gear in 0.166 s performs a complete revolution, then the angle of the faulty tooth with respect to the reference point of the tacho meter signal may be obtained as

$$\theta = 2\pi(0.064/0.166) = 2.42 \text{ rad}. \tag{42}$$

On the other hand, having the number of teeth on the gear ($N = 32$), the number representing the cracked tooth, with respect to the reference point on the gear, n_c, can be obtained as

$$n_c = N(2.42/2\pi) = 12.32. \tag{43}$$

The above equation shows that the 13th tooth of the gear from the reference point is cracked.

8. Conclusions

As mentioned before, the multiresolution analysis equations of the multiwavelet systems are in the form of matrix equations and this is one of the main differences between the scalar wavelet

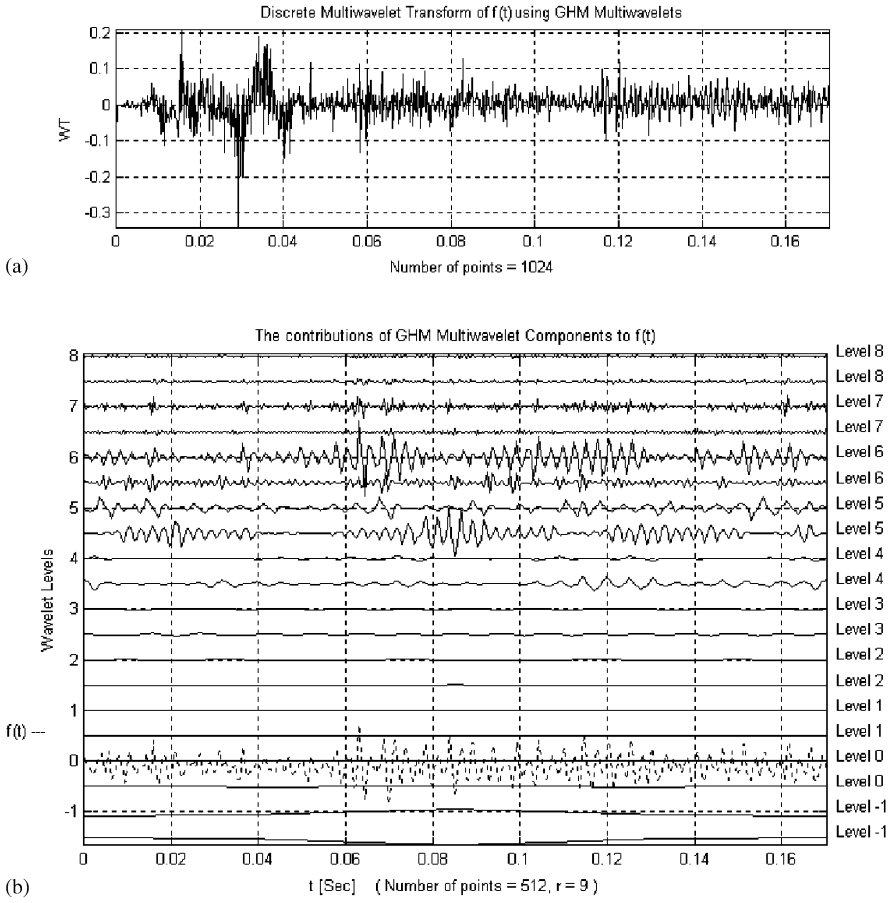

Fig. 8. Vibration signature analysis of the faulty gear using DGHM multiwavelet system [24]: (a) DGHM multiwavelet transform of the vibration signal; (b) decomposition of the signal into different levels of DGHM multiwavelet functions (- - -) $f(E)$; (c) three-dimensional mean-square map corresponding to the scale and wavelet functions of φ_1 and ψ_1 ($r = 9$); (d) three-dimensional mean-square map corresponding to the scale and wavelet functions of φ_2 and ψ_2 ($r = 9$); and (e) the compound three-dimensional mean-square map of all the scale and wavelet functions of φ_1, φ_2, ψ_1 and ψ_2 ($r = 9$).

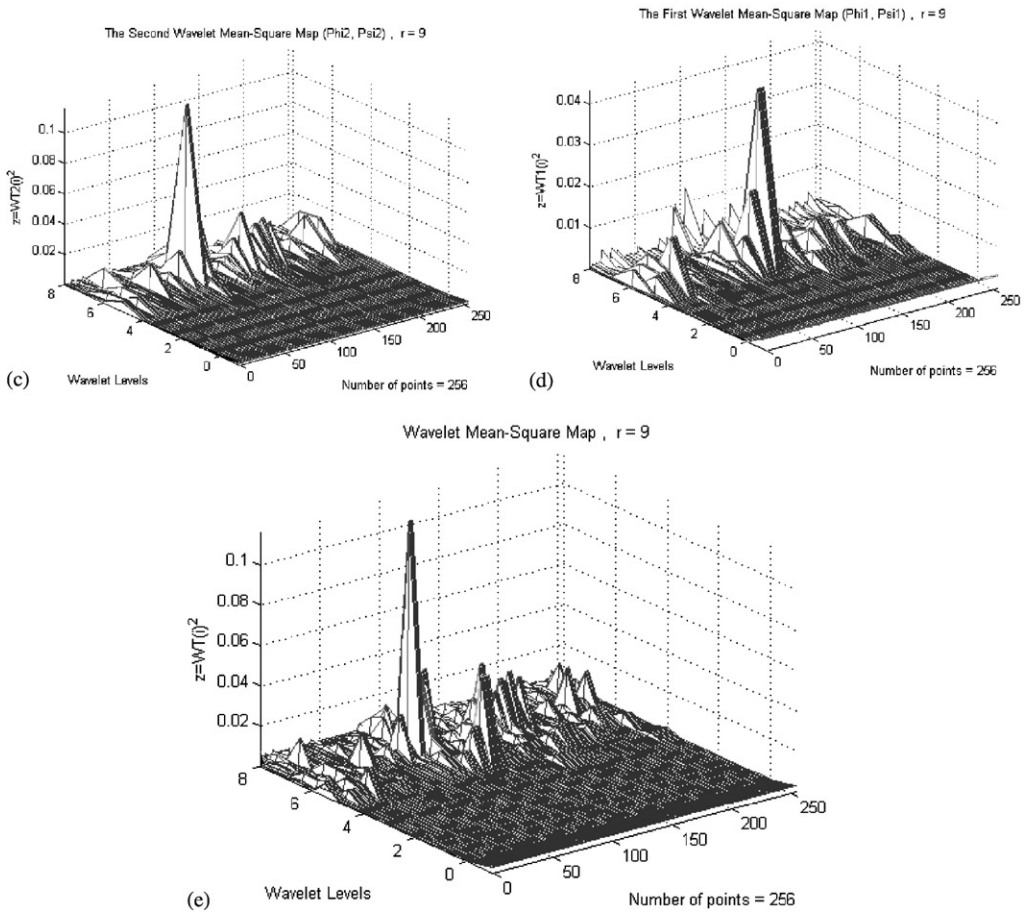

Fig. 8 (*continued*).

and the multiwavelet systems. On the other hand, considering the scalar wavelet systems, the signal space is generated only by translation and dilation of a single scale function and associated wavelet function. Then using the scalar wavelet systems to analyze a signal, the frequency band of the wavelet function at the higher scales will be very broad. In other words, the wavelet function spaces at higher scales are broadband, so that the frequency content of the narrow-band phenomena hidden in the signal that occur at relatively high frequencies, cannot be diagnosed precisely. This deficiency of the scalar wavelet systems can be overcome by dividing the frequency bands of different levels. Using the multiwavelet systems, one attains this achievement automatically, e.g., the DGHM multiwavelet system divides the frequency band of each level into two narrower frequency bands.

In order to apply the multiwavelet transform to a given signal, one needs to calculate the multiwavelet transform coefficients, but unlike the coefficients of the multiresolution analysis equation of scalar wavelet systems, the coefficients of the multiresolution analysis equation of the multiwavelet systems are matrices and need more complicated calculations. In this paper,

considering the method used to perform the scalar wavelet transform, the multiwavelet transform coefficients of an arbitrary signal $f(t)$ is obtained.

In order to examine the capability of the DGHM multiwavelet system for analysis of vibration signals, some artificial signals have been analyzed using the DGHM multiwavelet system. The results obtained through the analysis of the signals containing the transient phenomena, show that these phenomena appeared in the higher levels of the wavelet functions. Furthermore, since these phenomena have broad frequency bands, they may have components on several levels of the wavelet functions. Moreover, the results show that the DGHM multiwavelet system can be used to analyze the signals with a time-varying frequency as well as signals contaminated with the noise.

One of the main advantages of the wavelet analysis is that when analyzing the signal, the time location of any phenomenon existing in the signal is preserved, which is important for detecting the location of initial and local defects in mechanical systems.

In order to examine the ability of the DGHM multiwavelet system for practical fault detection of mechanical systems, the vibration signal of a gearing system with a cracked tooth has been analyzed. The results show that by using the multiwavelet system, one could detect the existing fault, as well as by having a tachometer signal as a reference, it is possible to determine the location of the cracked tooth.

The main point which should be emphasized here, is that the issue of wavelet analysis is a new area of research and is under development, and the multiwavelet systems is a quite new area of research among the other signal analysis techniques. Although many investigations have been performed recently on vibrational signal analysis using the scalar wavelet systems, no investigations have been reported on the applicability of multiwavelet systems to vibrational signal analysis. In this paper, the analysis of vibration signals using the multiwavelet system has been developed. Using the DGHM multiwavelet system, some simulated and experimental vibrational signals for a damaged mechanical system have been analyzed, and the local defects and the transient phenomena in the system extracted.

Acknowledgements

The authors wish to thank Professor R.B. Randall for supplying the experimental data for the faulty gearing system.

Appendix A. Nomenclature

$\mathbf{C}_l^j, \mathbf{D}_l^j$	multiwavelet transform coefficients vectors
c_l^j, d_l^j	elements of the vectors $\mathbf{C}_l^j, \mathbf{D}_l^j$
$f(t)$	signal in time domain
$\mathbf{G}_k$	coefficient matrix of multiresolution analysis equation used for obtaining the scale functions
$g_{i,j}^k$	elements of the coefficient matrix $\mathbf{G}_k$
$\mathbf{H}_k$	coefficient matrix of multiresolution analysis equation used for obtaining the wavelet functions

$h_{i,j}^k$	elements of the coefficient matrix $\mathbf{H}_k$
$\mathbf{I}$	identity matrix
i,j,k,l	integer numbers
$L^2(R)$	the space of the signals with a finite energy
N	the number of teeth of the gear
n_c	the cracked tooth number with respect to the reference point on the gear
t	time parameter
V_j	the space spanned by translation and dilation of the scale functions at scale j
W_j	the space spanned by translation and dilation of the wavelet functions at scale j
Z	the set of integer numbers
δ_{ij}, δ_n	Kronecker delta
$\mathbf{\Phi}$	a vector-valued function with the scale functions as its elements
φ_i	ith scale function
θ	the angle of the faulty tooth with respect to the reference point on the gear
$\mathbf{\Psi}$	a vector-valued function with the multiwavelet functions as its elements
ψ_i	ith wavelet function

References

[1] I. Daubechies, The wavelet transform, time-frequency localization and signal analysis, IEEE Transactions on Information Theory 36 (1990) 961–1005.
[2] S. Mallat, AWavelet Tour of Signal Processing, Academic Press, New York, 1998.
[3] C.S. Burrus, R.A. Gopinath, H. Guo, Introduction to Wavelets and Wavelet transforms, Prentice-Hall, Englewood Cliffs, NJ, 1998.
[4] J.S. Geronimo, D.P. Hardin, P.R. Massopust, Fractal functions and wavelet expansions based on several scaling functions, Journal of Approximation Theory 78 (1994) 373–401.
[5] G. Strang, V. Strela, Short wavelets and matrix dilation equations, IEEE Transactions on Signal Processing 43 (1995) 108–115.
[6] G.C. Donovan, J.S. Geronimo, D.P. Hardin, P.R. Massopust, Construction of orthogonal wavelets using fractal interpolation functions, SIAM Journal of Mathematical Analysis 27 (1996) 1158–1192.
[7] D.E. Newland, Wavelet analysis of vibration, Part 1: theory, Journal of Vibration and Acoustics 116 (1994) 409–416.
[8] D.E. Newland, Wavelet analysis of vibration, Part 2: wavelet maps, Journal of Vibration and Acoustics 116 (1994) 417–425.
[9] S.T. Lin, P.D. McFadden, Vibration analysis of gearboxes by the linear wavelet transform, Second International Conference on Gearbox Noise, Vibration, and Diagnostics, IMechE Conference Transactions, 16–17 November, 1995, pp. 59–72.
[10] Yulin Yan, Taro Shimogo, The application of Haar transform in signature extraction and condition monitoring of mechanical systems, JSME International Journal, Series III 33 (1990) 191–197.
[11] G.Y. Luo, D. Osypiw, M. Irle, Real-time condition monitoring by significant and natural frequencies analysis of vibration signal with wavelet filter and autocorrelation enhancement, Journal of Sound and Vibration 236 (2000) 413–430.
[12] K. Mori, N. Kasashima, T. Yoshiola, Y. Ueno, Prediction of spalling on a ball bearing by applying the discrete wavelet transform to vibration signals, Wear 195 (1996) 162–168.
[13] R. Ghanem, F. Romeo, A wavelet-based approach for the identification of linear time-varying dynamical systems, Journal of Sound and Vibration 234 (2000) 555–576.

[14] X.-G. Xia, J.S. Geronimo, D.P. Hardin, B.W. Suter, Design of prefilters for discrete multiwavelet transforms, IEEE Transactions on Signal Processing 44 (1996) 25–35.
[15] M. Cotronei, L.B. Montefusco, L. Puccio, Multiwavelet analysis and signal processing, Transactions on Circuits and Systems—II: Analog and Digital Signal Processing 45 (1998) 970–987.
[16] D.P. Hardin, D.W. Roach, Multiwavelet prefilters—I: orthogonal prefilters preserving approximation order $p \leqslant 2$, IEEE Transactions on Circuits and Systems—II: Analog and Digital Signal Processing 45 (1998) 1106–1112.
[17] T.R. Downie, B.W. Silverman, The discrete multiple wavelet transform and thresholding methods, IEEE Transactions on Signal Processing 46 (1998) 2558–2561.
[18] X.-G. Xia, B.W. Suter, Vector-valued wavelets and vector filter banks, IEEE Transactions on Signal Processing 44 (1996) 508–518.
[19] I.W. Selesnick, Balanced GHM-like multiscaling functions, IEEE Signal Processing Letters 6 (1999) 111–112.
[20] V. Strela, P.N. Heller, G. Strang, P. Topiwala, C. Heil, The application of multiwavelet filterbanks to image processing, IEEE Transactions on Image Processing 8 (1999) 548–563.
[21] Ivan W. Selesnick, Multiwavelet bases with extra approximation properties, IEEE Transactions on Signal Processing 46 (1998) 2898–2908.
[22] Ivan W. Selesnick, Interpolating multiwavelet bases and the sampling theorem, IEEE Transactions on Signal Processing 47 (1999) 1615–1621.
[23] T.D. Bui, G. Chen, Translation-invariant denoising using multiwavelets, IEEE Transactions on Signal Processing 46 (1998) 3414–3420.
[24] M. Rezaee, Analytical Development and Experimental Examination of Vibration Signature Analysis for Fault Detection by Designing the Biorthogonal Wavelet and Multiwavelet Systems, Ph.D. Thesis, Tarbiat Modarres University, Tehran, Iran, 2001.